



## MAGNETO-STRUCTURAL CORRELATIONS FOR THE $S = 1$ ALTERNATING CHAIN $[\{\text{Ni}_2(\text{dpt})_2(\mu\text{-N}_3)(\mu'\text{-N}_3)_2\}_n](\text{ClO}_4)_n$

R. VICENTE\* and A. ESCUER

Departament de Química Inorgànica, Universitat de Barcelona, Diagonal 647, 08028 Barcelona, Spain.

(Received 23 September 1994; accepted 16 December 1994)

**Abstract**—The magnetic behaviour of the  $S = 1$  alternating chain  $[\{\text{Ni}_2(\text{dpt})_2(\mu\text{-N}_3)(\mu'\text{-N}_3)_2\}_n](\text{ClO}_4)_n$  [dpt = bis(3-aminopropyl)amine] has been studied. The alternance in the  $J$  parameters is derived from the regular alternance in the structure of double and single bridges between the nickel(II) atoms along the chain. The susceptibility measurements between 4 and 300 K show strong antiferromagnetic coupling. The magnetic behaviour of this compound is correlated to the bond parameters by using MO extended-Hückel calculations and it is postulated that, in the title compound, the single bridge is more effective in propagating magnetic exchange than the double bridge.

The azido ligand provides an efficient superexchange pathway between paramagnetic ions such as nickel(II) in dinuclear,<sup>1,8</sup> tetranuclear,<sup>9</sup> one-dimensional<sup>10,14</sup> or two-dimensional<sup>15</sup> compounds. As a general trend, the polymeric compounds in which the azido ligand is coordinated in the end-to-end mode are always antiferromagnetically coupled. From the structural point of view and centring our scope in the one-dimensional nickel-(end-to-end) azido systems, a great variety of structural forms has been characterized recently. (a) Compounds with the generic formula  $\text{trans-}[\{\text{Ni}(\text{L})(\mu\text{-N}_3)\}_n](\text{ClO}_4)_n$ , in which L is cyclam, hexamethylcyclam (*meso*-CTH) or open tetra-amines.<sup>11-13</sup> These compounds are uniform  $\text{trans-}(\text{—N}_3\text{—NiL—N}_3\text{—})_n$  chains. (b)  $\text{cis-}[\{\text{Ni}(\text{333-tet})(\mu\text{-N}_3)\}_n](\text{PF}_6)_n$  333-tet = *N,N'*-bis(3-aminopropyl)-1,3-propanediamine, another uniform  $(\text{—N}_3\text{—NiL—N}_3\text{—})_n$  system but with the unprecedented *cis* coordination of the azide bridging ligand.<sup>14</sup> (c)  $\text{trans-}[\{\text{Ni}(\text{333-tet})(\mu\text{-N}_3)\}_n](\text{ClO}_4)_n$ ,<sup>14</sup> which presents the extremely unusual  $(\text{—NiL—(N}_3\text{)—NiL—(N}_3\text{)—})_n$  scheme along the chain axis, in which the azido ligand presents two

sets of bond distances and angles for azido-azido\*, being the first example of a structurally alternating monobridged  $\mu$ -azido chain. (d)  $[\{\text{Ni}_2(\text{dpt})_2(\mu\text{-N}_3)(\mu'\text{-N}_3)_2\}_n](\text{ClO}_4)_n$  [dpt = bis(3-aminopropyl)amine], also a structural and magnetic alternating  $(\text{—(N}_3\text{)—NiL—(N}_3\text{)}_2\text{—NiL—})_n$  chain.<sup>10</sup> These structural possibilities are summarized in Fig. 1.

Recently, a model to correlate the magnetic properties of the antiferromagnetic end-to-end nickel-azido systems has been proposed by the authors and successfully applied to cases (a)–(c).<sup>8,12,14</sup> For the title compound, previously reported from the crystallographic point of view,<sup>10</sup> the alternation in the single-double azido bridge implies an alternation in the  $J$  coupling parameters and this chain should be analysed by a theoretical model which takes into account this feature in the study of the magnetic interactions along the chain. The theoretical treatment for this kind of system based on the Hamiltonian  $H = -J\Sigma(S_{2i} \cdot S_{2i-1} + \alpha S_{2i} \cdot S_{2i+1})$  is well known for local  $S = 1/2$  Heisenberg chains,<sup>16</sup> but has only recently been reported<sup>17</sup> for local  $S = 1$  analogous systems. At this point, the analytic expression and the magneto-structural correlations can be applied to fill the lack of global magnetic characterization of the alternating single-double azido bridged compound  $[\{\text{Ni}_2(\text{dpt})_2(\mu\text{-N}_3)(\mu'\text{-N}_3)_2\}_n](\text{ClO}_4)_n$ .

\* Author to whom correspondence should be addressed.

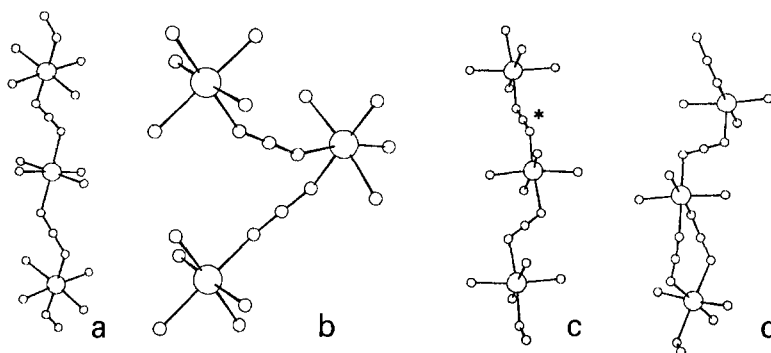


Fig. 1. Structural kinds of end-to-end 1-D nickel-azido systems reported to date. From the magnetic point of view, compound types a and b are homogeneous chains, whereas compounds c and d correspond to alternating systems. Alternance for c is due to different bond parameters for neighbouring azido-azido\* bridges.

## EXPERIMENTAL

### Synthesis

$[\{\text{Ni}_2(\text{dpt})_2(\mu\text{-N}_3)(\mu'\text{-N}_3)_2\}_n](\text{ClO}_4)_n$  was prepared and characterized as described previously.<sup>10</sup>

### Magnetic measurements

Magnetic measurements were carried out in the 4–300 K temperature range, as described previously.<sup>10</sup>

## RESULTS AND DISCUSSION

### Description of the structure

The structure of  $[\{\text{Ni}_2(\text{dpt})_2(\mu\text{-N}_3)(\mu'\text{-N}_3)_2\}_n](\text{ClO}_4)_n$  was published previously,<sup>10</sup> but some relevant aspects closely related with the superexchange pathways should be described. The structure consists of a 1-D  $-\text{Ni}-(\text{N}_3)_2-\text{Ni}-(\text{N}_3)-$  system, isolated by  $\text{ClO}_4^-$  anions. The  $[\{\text{Ni}_2(\text{dpt})_2(\mu\text{-N}_3)(\mu'\text{-N}_3)_2\}_n]^+$  chains can be considered as a built up from dinuclear  $\text{Ni}_2(\mu\text{-N}_3)_2(\text{dpt})_2$  units joined by  $\mu\text{-N}_3$  bridging ligands (Fig. 2.). The main bond parameters that influence the magnetic properties can be summarized as follows:  $\text{Ni}-\text{N}(1) = 2.194(4)$  Å,  $\text{Ni}-\text{N}(3') = 2.153(4)$  Å,  $\text{Ni}-\text{N}(4) = 2.143(4)$  Å,  $\text{Ni}-\text{N}(1)-\text{N}(2) = 128.2(3)^\circ$ ,  $\text{Ni}-\text{N}(3')-\text{N}(2') = 124.4(3)^\circ$ ,  $\text{Ni}-\text{N}(4)-\text{N}(5) = 119.2(3)^\circ$ , torsion angles  $\text{Ni}-\text{N}(1)-\text{N}(2)-\text{N}(3)-\text{Ni}' = 57.4^\circ$  and  $\text{Ni}-\text{N}(4)-\text{N}(5)-\text{N}(4')-\text{Ni} = 180.0^\circ$ .

The most interesting feature of this structure is the relative position of the two azido bridges in the  $\text{Ni}-(\mu\text{-N}_3)_2-\text{Ni}$  fragment. For pseudo-halogen-nickel(II) systems, in all the reported structures with double azido, cyanato, thiocyanato or seleno-

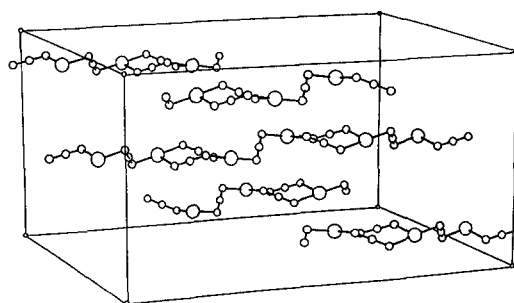
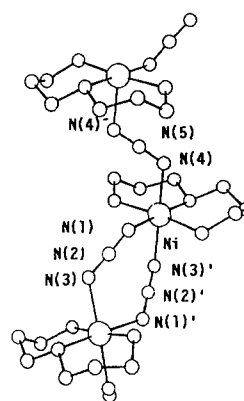


Fig. 2. Perspective view of  $[\{\text{Ni}_2(\text{dpt})_2(\mu\text{-N}_3)(\mu'\text{-N}_3)_2\}_n]^+$  showing the double-single azido bridge alternation and the cell packing of the nickel-azido skeleton of the chains.

cyanato bridges the two pseudo-halides are always parallel with the metal ions in the same plane, giving a pseudo-planar eight-membered ring, or it exists in a chair arrangement derived from a symmetric out-of-plane displacement of the metallic centres as is schematized in Fig. 3a (distortion type  $\delta$ ), in which  $\delta$  is defined as the dihedral angle between the  $xy$  plane and the  $\text{N}-\text{Ni}-\text{N}$  plane. In the  $\delta$  distortion the position of the six nitrogen atoms of

the azido bridges remains invariable. In the case of the compound  $[\{\text{Ni}_2(\text{dpt})_2(\mu\text{-N}_3)(\mu'\text{-N}_3)_2\}_n](\text{ClO}_4)_n$  the structure of the  $\text{Ni}-(\mu\text{-N}_3)_2\text{-Ni}$  fragment derives from the symmetric rotation of the coordination polyhedra of the nickel atoms around the  $x$ -axis, as shown in Fig. 3b. As a result of this movement, the nickel atoms and the central nitrogen atoms of the azido groups,  $\text{N}^*$ , are always maintained in the plane  $xy$ , whereas the  $\text{N}(\text{azido})$  atoms linked to the nickel atoms,  $\text{N}$ , go out of the original plane (distortion type  $\tau$ ),  $\tau$  being the angle defined for the  $\text{N}^*\text{-N}$  axis and the  $xy$  plane. For the title compound the corresponding mean  $\tau$  angle is roughly  $20^\circ$ .

#### Magnetic measurements

The molar magnetic susceptibility for a polycrystalline sample of  $[\{\text{Ni}_2(\text{dpt})_2(\mu\text{-N}_3)(\mu'\text{-N}_3)_2\}_n](\text{ClO}_4)_n$  is plotted vs the temperature in Fig. 4. The  $\chi_M$  value ( $6.28 \times 10^{-3} \text{ cm}^3 \text{ mol}^{-1}$  at room temperature) increases as the temperature

decreases, reaching a broad maximum at *ca* 115 K, with a  $\chi_M$  value of  $8.10 \times 10^{-3} \text{ cm}^3 \text{ mol}^{-1}$ . This maximum clearly indicates strong anti-ferromagnetic coupling between the  $\text{Ni}(\text{II})$  ions through the  $\text{N}_3$  bridge. Below this temperature, the susceptibility decreases continuously and reaches the minimum value of  $1.12 \times 10^{-3} \text{ cm}^3 \text{ mol}^{-1}$  at 7 K.

In a first approach, experimental data were fitted up to near the maximum (110 K) to the Weng equation<sup>18</sup> for uniform chains, based in the Hamiltonian  $H = -JS_i \cdot S_{i+1}$ . The best parameters so obtained were  $J = -62.4 \text{ cm}^{-1}$  and  $g = 2.39$ . The high  $J$  value indicates a good mean superexchange pathway.

The coupling parameters have been optimized up to 45 K from the equation<sup>17</sup> for an alternating chain based on the Hamiltonian  $H = -J\Sigma(S_{2i} \cdot S_{2i-1} + \alpha S_{2i} \cdot S_{2i+1})$ :

$$\chi_M = (2Ng^2\mu_B^2/3kT)/(X_r T_r)$$

in which

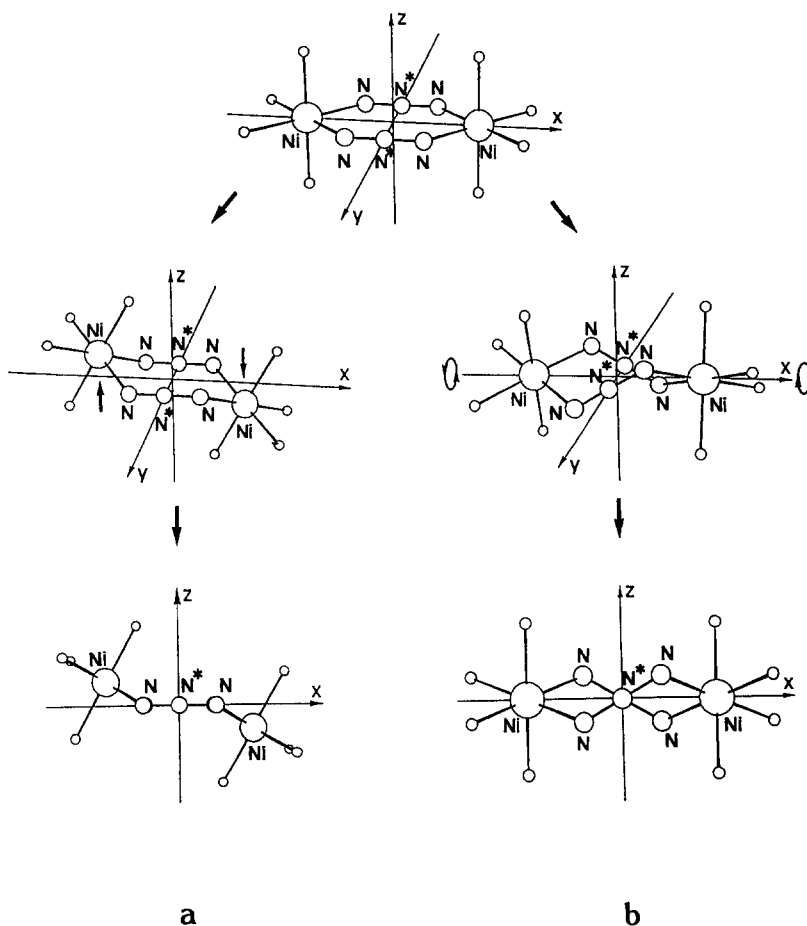


Fig. 3. Schematic representation for the two types of distortion found from planar  $(\mu\text{-N}_3)_2[\text{Ni}_2(\text{L})_4]$  entities:  $\delta$  type (left) and  $\tau$  type (right).

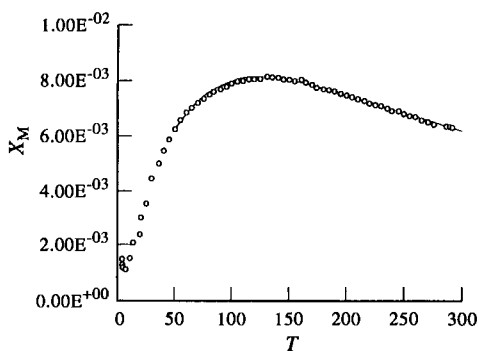


Fig. 4. Molar magnetic susceptibility ( $\text{cm}^3 \text{mol}^{-1}$ ) vs  $T$  (K) plot of polycrystalline sample of  $[\{\text{Ni}_2(\text{dpt})_2(\mu\text{-N}_3)(\mu'\text{-N}_3)_2\}_n](\text{ClO}_4)_n$ . Solid line shows the best fit obtained from the equation for an alternating chain.

$$(X_r T_r) = (A \cdot T_r^2 + B \cdot T_r + C) / (T_r^3 + D \cdot T_r^2 + E \cdot T_r + F),$$

with  $T_r = kT/|J|$  and  $A$ – $F$  polynomial expressions of the  $\alpha$  alternance parameter with the general form  $Z = z_0\alpha + z_1\alpha + z_2\alpha^2$ . Two sets of parameters  $A$ – $F$  for  $0 \leq \alpha \leq 0.5$  and  $0.5 \leq \alpha \leq 1$  should be used. This equation can reproduce the experimental data up to the temperature  $kT/|J| \approx 0.4$ . For the  $\alpha = 0$  value, dimeric behaviour is obtained, whereas for  $\alpha = 1$  uniform chain behaviour is observed.

The values corresponding to minimum in the regression are  $J = -84.6 \text{ cm}^{-1}$ ,  $J' = -41.4 \text{ cm}^{-1}$  ( $\alpha = 0.49$ ),  $g = 2.36$  with  $R = 4.23 \times 10^{-5}$  being the quality factor defined as  $R = \Sigma(\chi_{\text{Mcalc}} - \chi_{\text{Mobs}})^2 / \Sigma(\chi_{\text{Mobs}})^2$ . The generated curve of  $\chi_{\text{M}}$  vs  $T$  for this set of values can be seen in Fig. 4. The assignment of each of the two different  $J$  values at the two different kinds of bridges present in the chain is not immediately apparent and will be analysed in the next section.

#### Magneto-structural correlations

The chain  $[\{\text{Ni}_2(\text{dpt})_2(\mu\text{-N}_3)(\mu'\text{-N}_3)_2\}_n]^+$  can be considered as being built up from dinuclear  $\text{Ni}_2(\mu\text{-N}_3)_2(\text{dpt})_2$  units joined by  $\mu\text{-N}_3$  bridging ligands (Fig. 2). Consequently, the magnetic behaviour can be studied as the result of the behaviour of two different fragments: one monobridged  $\text{Ni}\text{—N}_3\text{—Ni}$  and one bibriged  $\text{Ni}\text{—}(\text{N}_3)_2\text{—Ni}$  entity.

For an  $[\text{NiNi}]$  system, the antiferromagnetic component of  $J$  is a function of  $\Delta^2(xy) = |E\Phi_{xy(s)} - E\Phi_{xy(a)}|^2$  and  $\Delta^2(z^2) = |E\Phi_{z^2(s)} - E\Phi_{z^2(a)}|$ , with  $\Sigma\Delta^2 = \Delta^2(xy) + \Delta^2(z^2)$  directly related to the antiferromagnetic component of  $J$ .<sup>19</sup> The previously reported model showed that the antiferromagnetic component of  $J$  is strongly dependent on the

$\text{Ni}\text{—N—N}$  and the  $\text{Ni}\text{—N—N—N—Ni}$  torsion angles, whereas it is only slightly dependent on the  $\text{Ni}\text{—N}$  bond, with distances typically in the 2.12–2.18 Å range. For the monobridged fragment of the title compound, MO calculations were performed on the same model used in previous works<sup>12, 14</sup> (a dimeric  $[\text{N}_3(\text{NH}_3)_4\text{Ni}\text{—N}_3\text{—Ni}(\text{NH}_3)_4\text{N}_3]^+$  fragment) by using the experimental structural data:  $\text{Ni}\text{—N}$  distances 2.10 Å,  $\text{N}\text{—N}$  distances 1.17 Å,  $\text{Ni}\text{—N—N}$  angle  $119.2^\circ$  and  $\text{Ni}\text{—N}_3\text{—Ni}$  torsion angle  $180^\circ$ , allowing one to calculate  $\Sigma\Delta^2 = 0.314 \text{ eV}^2$ .

The dinuclear  $\text{Ni}\text{—}(\text{N}_3)_2\text{—Ni}$  fragment of the  $[\{\text{Ni}_2(\text{dpt})_2(\mu\text{-N}_3)(\mu'\text{-N}_3)_2\}_n]^+$  chain needs specific MO extended-Hückel calculations to correlate the structural and magnetic data. Very recently, magneto-structural correlations between the dihedral angle  $\delta$  and the magnetic coupling for dinuclear complexes of nickel(II) with two azides as bridging ligands and  $\delta$  distortion have been reported.<sup>8</sup> In this model (Fig. 5a), the two nickel atoms rotate freely around the axis determined by the two terminal nitrogen atoms of the two bridging azide ligands, from planar to chair conformation.

The results of this study cannot be extrapolated to the dinuclear entity  $\text{Ni}\text{—}(\text{N}_3)_2\text{—Ni}$  in

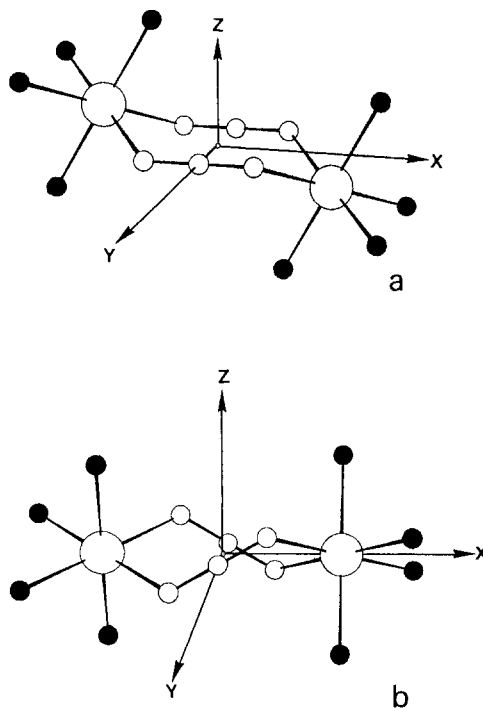


Fig. 5. Model of the  $(\mu\text{-N}_3)_2[\text{NiNi}]$  fragments used in the MO calculations. Black balls schematize  $\text{NH}_3$  groups. Constant parameters: all the  $\text{Ni}\text{—N}$ , 2.10 Å;  $\text{N}\text{—N}$  (azido), 1.17 Å. Variable parameters:  $\text{Ni}\text{—N—N}$  angle and  $\text{Ni}\text{—N—N—N—Ni}$  torsion as a function of the corresponding  $\delta$  and  $\tau$  parameters.

$[\{\text{Ni}_2(\text{dpt})_2(\mu\text{-N}_3)(\mu'\text{-N}_3)_2\}_n](\text{ClO}_4)_n$ , since its geometry arises not from the  $\delta$  distortion but from the  $\tau$  distortion. Thus, extended-Hückel MO calculations have been performed by means of the CACAO program<sup>20</sup> on a dinuclear fragment modelled as in Fig. 5b. The calculations were made by varying the  $\tau$  angle, defined as the  $\text{N}^*\text{-N}-(xy \text{ plane})$  angle, and maintaining as constant the distances:  $\text{Ni-NH}_3 = 2.10 \text{ \AA}$ ,  $\text{Ni-N}(\text{azido}) = 2.10 \text{ \AA}$  and  $\text{N-N} = 1.17 \text{ \AA}$ . For  $\tau = 0$ , the  $\text{Ni-N-N}$  angle is  $135^\circ$  and the  $\text{N}^*\text{-N}^*$  distance  $2.96 \text{ \AA}$ . Atomic parameters used were standard for the program. The corresponding Walsh diagram for  $\tau$  angles between  $0$  and  $60^\circ$  is shown in Fig. 6a. For comparative purposes, the Walsh diagram for  $\delta$  angles varying between  $0$  and  $60^\circ$  ( $\delta$  distortion model) is plotted in Fig. 6b.

The values of  $\Sigma\Delta^2$  vs the  $\delta$  or  $\tau$  angles for the two possible patterns are plotted in Fig. 6c. For the  $\tau$  distortion,  $\Sigma\Delta^2$  has a maximum at  $\tau = 0$ , decreases quickly with increase in  $\tau$  reaching the  $\Sigma\Delta^2 = 0$  value at  $\tau = 32^\circ$ , and subsequently increases slowly. This behaviour is different from that found for the  $\delta$  distortion, for which  $\Sigma\Delta^2$  decreases continuously in the interval  $\delta = 0\text{--}60^\circ$  to reach the zero value at  $\delta = 90^\circ$ , which is chemically unlikely due to steric hindrance. On the contrary, for the  $\tau$  distortion, the geometry associated with the  $\tau$  angle of approximately  $32^\circ$  is reasonable.

The dinuclear entity  $\text{Ni}-(\text{N}_3)_2\text{-Ni}$  in  $[\{\text{Ni}_2(\text{dpt})_2(\mu\text{-N}_3)(\mu'\text{-N}_3)_2\}_n](\text{ClO}_4)_n$  is slightly asymmetric, and the mean  $\tau$  value is roughly  $20^\circ$ . For this angle, the calculated  $\Sigma\Delta^2$  value is  $0.130$ . The ratio of the  $\Sigma\Delta^2$  values for the dinuclear entities  $\text{Ni}-(\text{N}_3)_2\text{-Ni}$  and  $\text{Ni-N}_3\text{-Ni}$  is consequently  $0.130/0.314 = 0.42$ , in good agreement with the  $\alpha$  value of  $0.49$  found in the fit of the experimental data. This result permits the assignment of the

$-84.6 \text{ cm}^{-1}$   $J$  value to the single azido bridge and the  $\alpha J$  value of  $-41.4 \text{ cm}^{-1}$  to the double azido bridge.

The accuracy of this correlation can be understood only as a qualitative approximation. Several factors such as the method of calculation (extended-Hückel) and more complicated modelling may be improved. On the other hand, the fit of the experimental susceptibility data in which the number of adjustable parameters is high can lead to different sets of parameters in good agreement with the experiment, even with absurd values for one or more of them which should be discarded. The final choice should be dictated by the agreement with parameters for interactions in similar and unambiguously assigned compounds. In this way, previously reported nickel(II) azido dinuclear species or chains are a good reference. Values of  $\Sigma\Delta^2$  close to  $0.130$  have been found for  $[\text{Ni}(\text{L})(\mu\text{-N}_3)]_n(\text{ClO}_4)_n$  compounds, in which L is cyclam or 232-tet and the corresponding low  $J$  values are  $-39.2$  and  $-26.7 \text{ cm}^{-1}$ . For L = 323-tet,  $\Sigma\Delta^2$  is  $0.207$  and the corresponding  $J$  value is  $-62.7 \text{ cm}^{-1}$ .

Other possible references for comparison are the dinuclear compounds with  $\delta$  distortion described in the literature: according to the data of Fig. 6c, the  $J$  parameter for the double bridge of the title compound ( $\tau = 20^\circ$ ) should be equivalent to that obtained for a dinuclear system with  $35^\circ$  of  $\delta$  distortion. To our knowledge this compound has not been reported to date, but the  $\alpha J$  value for the title compound ( $-41.4 \text{ cm}^{-1}$ ) is intermediate, as expected, between the data provided<sup>8</sup> for  $(\mu\text{-N}_3)_2[\text{Ni}(\text{en})_2](\text{PF}_6)_2$  ( $\delta = 45^\circ$ ,  $J = -4.6 \text{ cm}^{-1}$ ) and  $(\mu\text{-N}_3)_2[\text{Ni}(\text{tren})_2](\text{PF}_6)_2$  ( $\delta = 20.7^\circ$ ,  $J = -70 \text{ cm}^{-1}$ ).

The agreement with the published values reinforces the result obtained previously

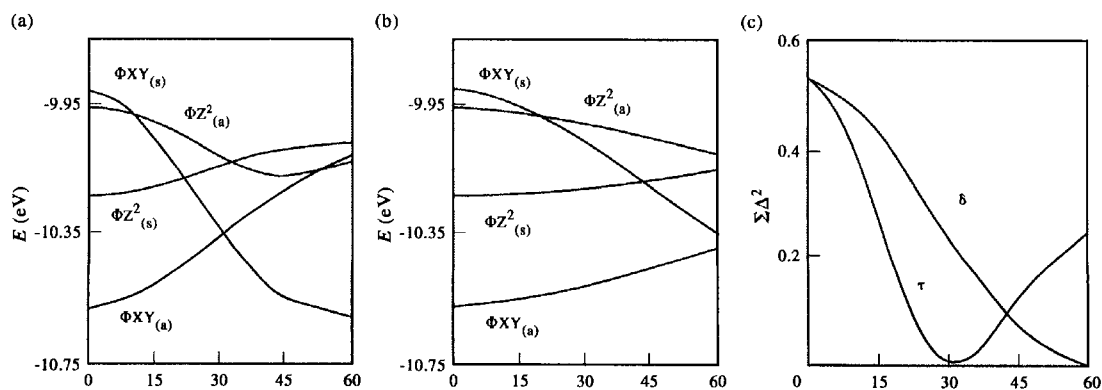


Fig. 6. (a) MO correlation diagram for a  $(\mu\text{-N}_3)_2[\text{NiNi}]$  system as a function of the symmetrical variation of the  $\tau$  angle. (b) MO correlation diagram for a  $(\mu\text{-N}_3)_2[\text{NiNi}]$  system as a function of the symmetrical variation of the  $\delta$  angle. (c) Plot of  $\Sigma\Delta^2$  vs  $\tau$  or  $\delta$  for a  $(\mu\text{-N}_3)_2[\text{NiNi}]$  system.

for  $[\{\text{Ni}_2(\text{dpt})_2(\mu\text{-N}_3)(\mu'\text{-N}_3)_2\}_n](\text{ClO}_4)_n$  from extended-Hückel MO calculations, in which the most efficient superexchange pathway is assigned to the single bridge and the less efficient to the double bridge due to the corresponding structural parameters.

*Acknowledgements*—This work was financially supported by the Comisión Interministerial de Ciencia y Tecnología PB93-0772.

## REFERENCES

1. F. Wagner, M. T. Mocella, M. J. D'Aniello, A. H. J. Wang and E. K. Barefield, *J. Am. Chem. Soc.* 1974, **96**, 2625.
2. C. G. Pierpont, D. N. Hendrickson, D. M. Duggan, F. Wagner and E. K. Barefield, *Inorg. Chem.* 1975, **14**, 604.
3. P. Chaudhuri, M. Guttman, D. Ventur, K. Wiegardt, B. Nuber and J. Weiss, *J. Chem. Soc., Chem. Commun.* 1985, 1618.
4. M. I. Arriortua, A. R. Cortes, L. Lezama, T. Rojo, X. Solans and M. Font-Bardía, *Inorg. Chim. Acta* 1990, **174**, 263.
5. A. Escuer, R. Vicente and J. Ribas, *J. Magn. Magn. Mater.* 1992, **110**, 181.
6. A. R. Cortes, J. I. Ruiz do Larramendi, L. Lezama, T. Rojo, K. Urriaga and M. I. Arriortua, *J. Chem. Soc., Dalton Trans.* 1992, 2723.
7. R. Vicente, A. Escuer, J. Ribas, M. S. El Fallah, X. Solans and M. Font-Bardía, *Inorg. Chem.* 1993, **32**, 1920.
8. J. Ribas, M. Monfort, C. Bastos, C. Diaz and X. Solans, *Inorg. Chem.* 1993, **32**, 3557.
9. J. Ribas, M. Monfort, R. Costa and X. Solans, *Inorg. Chem.* 1993, **32**, 695.
10. R. Vicente, A. Escuer, J. Ribas and X. Solans, *Inorg. Chem.* 1992, **31**, 1726.
11. A. Escuer, R. Vicente, J. Ribas, M. S. El Fallah and X. Solans, *Inorg. Chem.* 1993, **32**, 1033.
12. A. Escuer, R. Vicente, J. Ribas, M. S. El Fallah, X. Solans and M. Font-Bardía, *Inorg. Chem.* 1993, **32**, 3727.
13. A. Escuer, R. Vicente, M. S. El Fallah, J. Ribas, X. Solans and M. Font-Bardía, *J. Chem. Soc., Dalton Trans.* 1993, 2975.
14. A. Escuer, R. Vicente, J. Ribas, M. S. El Fallah, X. Solans and M. Font-Bardía, *Inorg. Chem.* 1994, **33**, 1842.
15. M. Monfort, J. Ribas and X. Solans, (a) *J. Chem. Soc., Chem. Commun.* 1993, 350; (b) *Inorg. Chem.* 1994, **33**, 742.
16. O. Kahn, *Molecular Magnetism*, VCH, New York (1993).
17. J. J. Borrás-Almenar, E. Coronado, J. Curely and R. Georges, *Inorg. Chem.*, accepted for publication (private communication); J. J. Borrás, PhD Thesis. Valencia, Spain (1992).
18. C. Y. Weng, PhD Thesis. Carnegie Institute of Technology (1968).
19. P. J. Hay, J. C. Thibeault and R. Hoffmann, *J. Am. Chem. Soc.* 1975, **97**, 4884.
20. C. Mealli and D. M. Proserpio, CACAO program (Computer Aided Composition of Atomic Orbitals). *J. Chem. Educ.* 1990, **67**, 339.